Design of an Airborne Portable Remote Imaging Spectrometer (PRISM) for the Coastal Ocean

P. Mouroulis, B. van Gorp, R. O. Green, D. Cohen, D. Wilson, D. Randall, J. Rodriguez, O. Polanco, K. Balasubramanian, R. Vargas, R. Hein, H. Sobel, M. Eastwood

Jet Propulsion Laboratory, California Institute of Technology, Pasadena, CA, 91109

H. Dierssen

Department of Marine Sciences, University of Connecticut Avery Point, Groton, CT 06340

Abstract: **PRISM is a pushbroom imaging spectrometer currently under development at the Jet Propulsion Laboratory, intended to address the needs of airborne coastal ocean science research. We describe here the instrument design and the technologies that enable it to achieve its distinguishing characteristics. PRISM covers the 350-1050 nm range with a 3.1 nm sampling and a 33^0 field of view. The design provides for high signal to noise ratio, high uniformity of response, and low polarization sensitivity. The complete instrument also incorporates two additional wavelength bands at 1240 and 1610 nm in a spot radiometer configuration to aid with atmospheric correction.**

I. INTRODUCTION

There is an important need in coastal ocean science for high spatial and temporal resolution spectral measurements to complement the capabilities of Earth-orbiting satellites. Airborne sensors such as PRISM provide on-demand monitoring of coastal areas to assess episodic events and also permit longer term monitoring at spatial scales that would be difficult to achieve from space. The benefits of such sensors will be found in 1) understanding the role of coastal habitats in human health and well-being, 2) assessing impacts of inland nutrient, sediment, and pollutant inputs on coastal zones, 3) supporting coastal management and ports operations, and 4) improving the monitoring and forecasting of acute and chronic natural and anthropogenic hazards such as large storms, tsunamis, toxic spills, and icebergs.

PRISM was conceived in response to a proposal call from NASA's Ocean Biology and Biogeochemsitry Program. Development was initiated in September 2009 and delivery is expected in 2012. After a calibration flight, the instrument will prove its utility through a planned investigation of eelgrass beds in the Elkhorn Slough area of Monterey Bay in California, followed by delivery to NASA to be made available for on-demand use by the Ocean Science community.

Sensors for Ocean Science measurements are distinguished from those used for land measurements by the fact that the reflectivity of water is generally low compared with the typical reflectivity of land targets. This leads to the requirement for achieving a high signal-to-noise ratio in the visible and near infrared range and minimizing the polarization dependence of the sensor transmission, in addition to a robust atmospheric correction strategy. The PRISM design responds to these challenges by utilizing several innovations including: 1) a design that minimizes the number of elements, maintains low angles of incidence on optical surfaces, allows large aperture (F/1.8), and minimizes distortions, and 2) a polarization-insensitive diffraction grating fabricated by electron-beam lithography. The system is enabled by a rapid snapshot readout detector array and specially developed low-noise readout electronics.

II. SPECIFICATIONS

PRISM integrates two independent instruments in one package: an imaging spectrometer covering the visible and near-infrared (VNIR) range, and a short-wave infrared (SWIR) spot radiometer. The basic specifications are given in Tables 1 and 2.

TABLE 1
SPECTROMETER SPECIFICATIONS

Spectral	Range	350-1050 nm
	Sampling	3.1 nm
Spatial	Field of view	33.1 deg
	Instantaneous FOV	0.95 mrad
	Spatial swath	610 pixels
	Spatial resolution	0.3-20 m
Radiometric	Range	0 – 75% R
	SNR	2000 @ 450 nm *
	Polarization variation	< 2%
Uniformity	Spectral cross-track	>95% **
	Spectral IFOV mixing	< 5% ***

*: at an equivalent 10 nm sampling and 12 fps, reference radiance R = 0.05, 45^o zenith angle
**: straightness of monochromatic slit image (pixel fraction)
***: registration of spectrum to array row (pixel fraction)

TABLE 2
SWIR SPECIFICATIONS

Spatial	FOF/IFOV	1.9x1.9 +/-0.1 mrad
Spectral	Channel 1 center	1240 nm
	Ch. 1 bandwidth	20 nm
	Channel 2 cener	1610 nm
	Ch. 2 bandwidth	60 nm
Radiometric	SNR	>350
	Ch. 1 ref. radiance	0.054 μW/cm^2 sr nm
	Ch. 2 ref. radiance	0.017 μW/cm^2 sr nm

III. OPTICAL DESIGN

The basic optical design of PRISM has been previously described [1]. It relies on the basic Dyson spectrometer form [2] which permits high optical throughput (F/1.8 in this case). The design utilized low angles of incidence on optical components (with the exception of one surface where light was totally internally reflected), a minimum number of optical components, and a specially designed grating groove profile to reduce polarization dependence. The design currently being implemented differs from the one described in [1] in three areas: 1) it utilizes a displaced slit to remove the need for high-quality anti-reflection coating on the array detector, 2) it adds an external window to seal the entire system in vacuum, and 3) it places the total internal the spectrometer utilizes the minimum number of optical components: a focusing lens and a grating. A raytrace of the system is shown in Fig. 1.

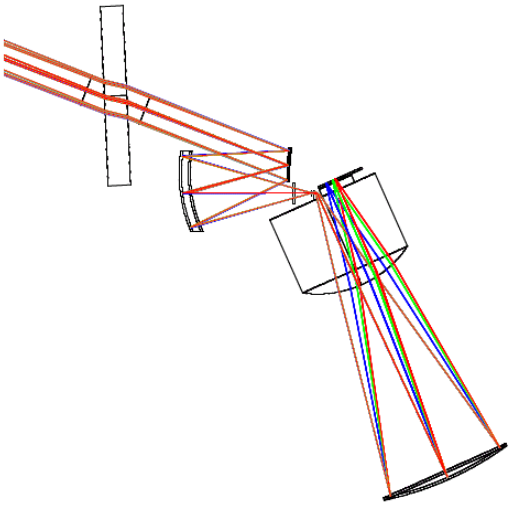

Fig. 1. Raytrace of the telescope/spectrometer system, showing the direction of dispersion.

Representative spot diagrams are shown in Fig. 2.

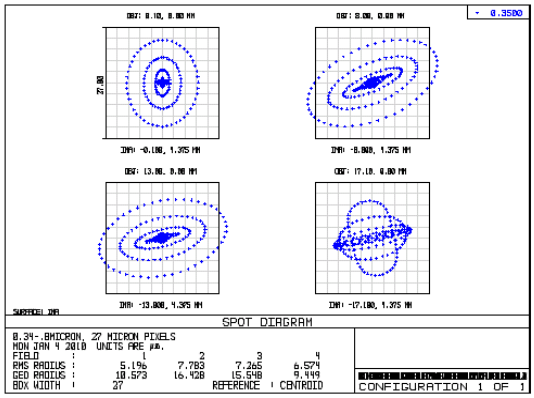

Fig.2. Spectrometer spot diagrams for four field positions at 350 nm. The box size is one pixel (27 µm).

The grating groove design is critical in achieving the reduced polarization sensitivity of the overall instrument. Gratings are fabricated through electron-beam lithography techniques developed at JPL [3]. We have implemented various test groove designs on flat substrates in order to check the agreement with theory. The agreement is very good and the overall sensitivity is within expectation for achieving the instrument-level goal. Figure 3 shows experimental results achieved with the simplest design, a triangle groove similar to that proposed in [1].

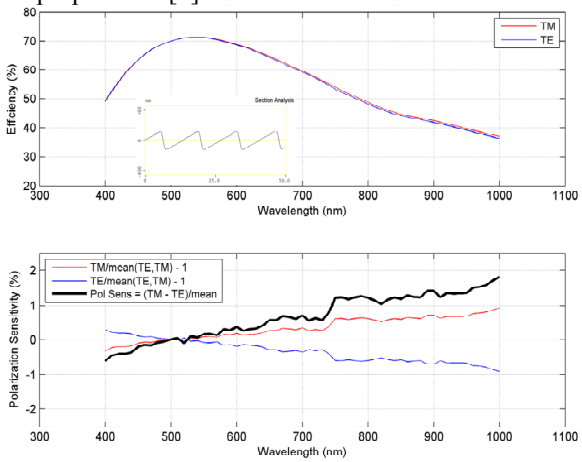

Fig. 3. Measured efficiency of triangular groove test grating and the difference between s and p components.

The overall polarization sensitivity of the system depends on the quality of the anti-reflection coatings on the refractive surfaces as well as the telescope mirror coatings. These have been optimized, in conjuction with the window angle to provide the best overall balance through the field. A complete system-level polarization computation accounting for all effects is shown in Fig. 4. It can be seen that the predicted polarization sensitivity stays below the specification of 2% throughout the wavelength range.

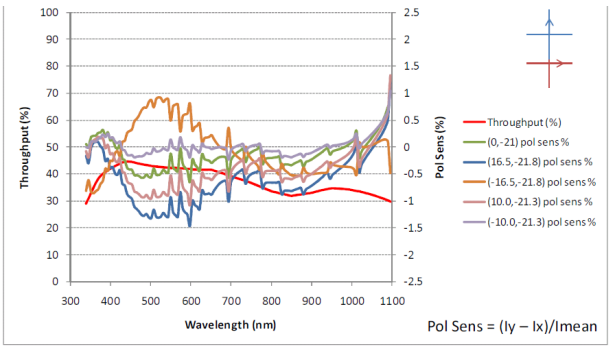

Fig. 4. Predicted polarization variation as a function of wavelength for various field positions. The incident polarization vectors are parallel and perpendicular to the slit. Other orientations give similar results.

The SWIR radiometer design comprises a 60mm F/2 cemented doublet for a telescope, a precision square pinhole aperture 0.12 x 0.12 mm, a collimating doublet after the pinhole, a dichroic beamsplitter, bandpass filters, and identical focusing doublets onto two InGaAs detectors of 0.3mm diameter. A schematic is shown in the next section.

IV. OPTO-MECHANICAL DESIGN

The telescope/spectrometer assembly and the SWIR radiometer are housed in a vacuum enclosure, the bottom plate of which is used for mounting both structures. This is shown in Fig. 5.

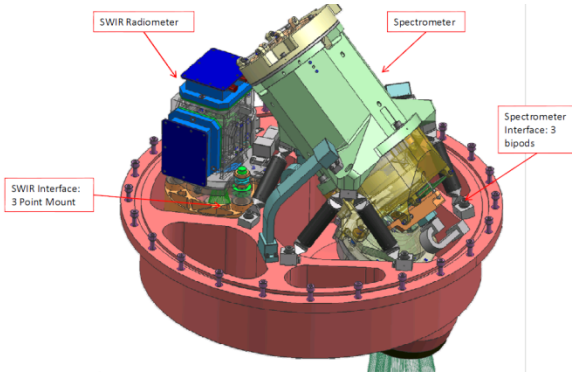

Fig. 5. Spectrometer and SWIR assembly mounted on plate. The outside diameter is 16".

The opto-mechanical design must respond to very tight stability requirements while also satisfying the difficult component placement arising from the proximity of detector and slit. The fabrication and assembly tolerances, (typically on the order of 50 µm in decenters) are achieved with an assembly technique that takes advantage of the rotational symmetry of both the telescope and the spectrometer designs. The stability requirements are driven by the desire to maintain spectral calibration knowledge through a deployment. The stability requirement is set at 0.1nm with a goal of 0.05 nm. Since one pixel (27 µm) corresponds to 3.1 nm, it follows that the spectrum registration must be stable relative to the detector to within ~0.4 µm. This requires a very stiff mechanical structure. The first mode frequency of the assembly is > 600Hz. The corresponding thermal stability is comparatively less stringent (1K). The nominal temperature of the entire system, including detectors, is 23° C. Thermal analysis indicates that the system reaches operational temperature within less than 2 hrs from turn-on for all expected outside conditions.

The telescope and spectrometer are assembled and pre-aligned as independent units, then brought together for a final adjustment that involves fine-tuning the detector position, grating clocking, and telescope focus relative to the slit. The detector assembly is adjustable in all six degrees of freedom in fine increments that are required to reach the 95% uniformity specification.

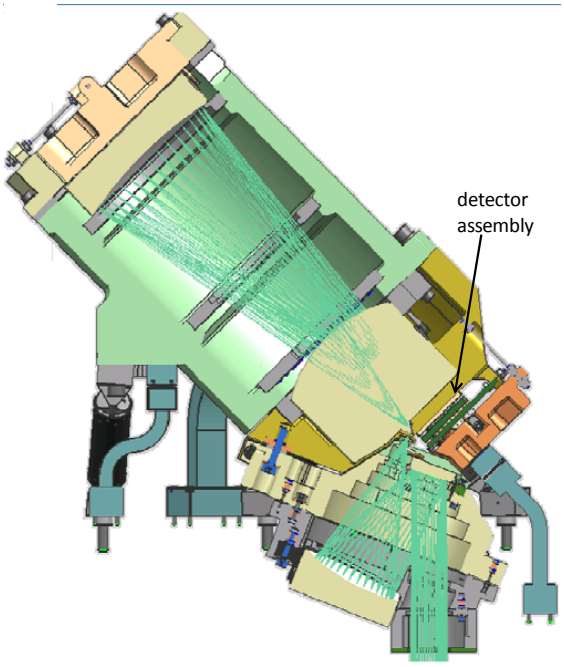

Fig. 6. Spectrometer/telescope and detector assembly in cross section, with light incident from the bottom.

The SWIR two-band radiometer is shown in Fig. 7. Its driving requirements are radiometric and boresight stability, which are achieved with a stiff structure and temperature control to within 1K.

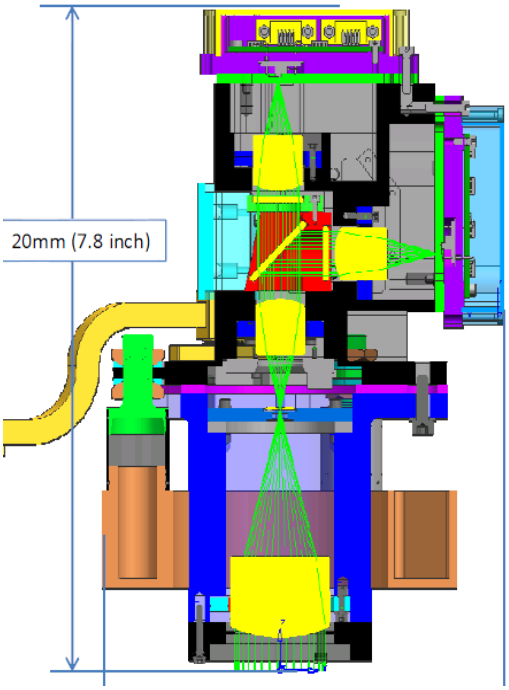

Fig. 7. SWIR radiometer opto-mechanical design.

The two InGaAs diode assemblies seen at the top and right of the picture are independently aligned and bonded in place. The SWIR boresight will be characterized during calibration relative to the spectrometer with an accuracy of 0.1 mrad.

V. FOCAL PLANE AND ELECTRONICS

The focal plane array (FPA) is a 640x480 format HyViSI® array from Teledyne that operates in snapshot readout mode, which is best suited for pushbroom systems due to the lack of image smear. The characteristics of this array including the A/R coating have been described in [4]. Only ~half of the 480 columns are used (230 spectral channels total). This allows rapid readout rate (200 Hz) and consequent expansion of dynamic range. The readout electronics are custom-built at JPL and have been tested previously with similar arrays. Fig. 8 shows the electronic system schematic.

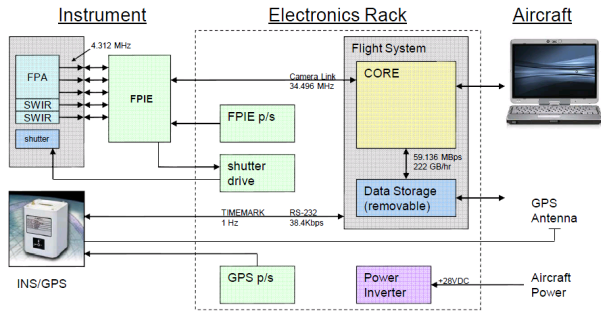

Fig. 8. Electronic control scheme

Data are digitized to 14 bits and output to a standard Camera Link interface. Removable data storage is used. Geolocation data are acquired and stored to ensure pointing knowledge within one IFOV.

Special attention has been paid to the SWIR electronics due to the very low signals expected (pA). A fully differential circuit has been implemented that reduces dark current to negligible levels, and an integrated thermoelectric cooler assembly is used for temperature stability. A breadboard circuit is currently under evaluation.

VI. CALIBRATION AND FLIGHT

PRISM will undergo thorough spectral, radiometric, and spatial calibration/characterization in the laboratory. Spectral and spatial response functions are derived for all channels across the field of view, with center and bandwidth knowledge to better than 0.1nm. Radiometric error budget shows that uncertainty within 1% is achievable. Signal and noise measurements will be performed at the specified reference radiances. The expected PRISM SNR is given in Fig. 9.

PRISM does not incorporate an on-board calibrator. In its place, a well-characterized integrating sphere fed by tungsten halogen lamps and two lasers will be used before take-off and after landing to confirm the stability of instrumental characteristics.

PRISM test flights will be on the Twin Otter aircraft which can fly without a port window. PRISM can be adapted for operation on other aircraft. However, attention must be paid to the effect of an additional window on polarization. Low polarization sensitivity cannot be maintained for a wide-field system through an arbitrary window configuration. Thus each new platform may require a custom window with appropriate antireflection coating.

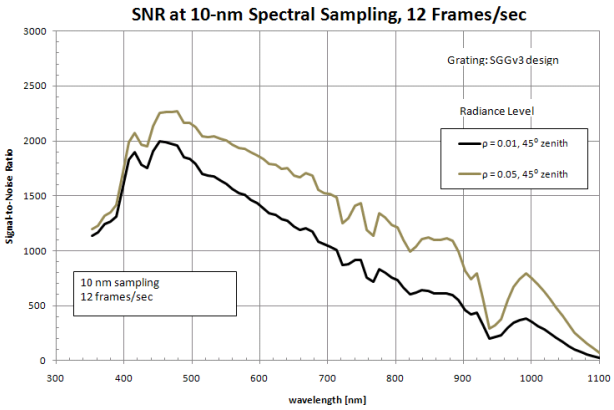

Fig. 9. Signal-to-noise ratio for two reference radiances

ACKNOWLEDGMENTS

This research has been performed at the Jet Propulsion Laboratory, California Institute of Technology, under a contract with the National Aeronautics and Space Administration. NASA programmatic support through ESTO, Airborne Science, and Ocean Biology and Biogeochemistry programs is gratefully acknowledged. The design has benefitted by comments from anonymous reviewers as well as P. Bontempi, M. Dudik, C. Fisher, S. Macenka, and J. Oseas. Bo-Cai Gao is advising us on atmospheric correction techniques.

REFERENCES

[1] P. Mouroulis, R. O. Green, and D. W. Wilson: "Optical design of a coastal ocean imaging spectrometer", Opt. Express vol. 16, pp. 9087-9095, 2008

[2] L. Mertz, "Concentric spectrographs", Appl. Opt. vol. 16, pp. 3122-3124, 1977

[3] D. W. Wilson, P. D. Maker, R. E. Muller, P. Mouroulis, and J. Backlund, "Recent advances in blazed grating fabrication by electron-beam lithography", Proc. SPIE vol. 5173, pp. 115-126, 2003

[4] Y. Bai et al, "Teledyne imaging sensors: Silicon CMOS imaging technologies for x-ray, UV, visible and near infrared", Proc. SPIE vol. 721, 702102, 2008